

Article

Application of ORC in a Distributed Integrated Energy System Driven by Deep and Shallow Geothermal Energy

Hongmei Yin ^{1,2}, Likai Hu ^{3,*}, Yang Li ^{1,*}, Yulie Gong ⁴, Yanping Du ⁵, Chaofan Song ¹  and Jun Zhao ¹

¹ Key Laboratory of Efficient Utilization of Low and Medium Grade Energy, Tianjin University, Ministry of Education of China, Tianjin 300350, China; yinhongmei@tju.edu.cn (H.Y.); songchaofan@tju.edu.cn (C.S.); zhaojun@tju.edu.cn (J.Z.)

² School of Environmental Science and Engineering, Tianjin University, Tianjin 300350, China

³ China Huadian Corporation Ltd. Tianjin Company, Tianjin 300203, China

⁴ Guangzhou Institute of Energy Conversion, Chinese Academy of Sciences, Guangzhou 510640, China; gongyl@ms.giec.ac.cn

⁵ China-UK Low Carbon College, Shanghai Jiao Tong University, Shanghai 200240, China; yanping.du@sjtu.edu.cn

* Correspondence: hulikai@tju.edu.cn (L.H.); liyangtju@tju.edu.cn (Y.L.)

Abstract: This study presents a distributed integrated energy system driven by deep and shallow geothermal energy based on forward and reverse cycle for flexible generation of cold, heat and electricity in different scenarios. By adjusting the strategy, the system can meet the demand of heat-electricity in winter, cool-electricity in summer and electricity in transition seasons. The thermodynamic analysis shows that the thermal efficiency of the integrated energy system in the heating and power generation mode is 16% higher than that in the cooling and power generation mode or the single power generation mode. Meanwhile, the annual heat-obtaining quantity of the system is reduced by 11% compared with that of the independent power generation system, which effectively alleviates the imbalance of the temperature field of the shallow geothermal reservoir. In terms of net power generation, the integrated energy system can generate approximately 31% more electricity than the conventional independent cooling and heating system under the same cooling and heating capacity. An integrated system not only realizes the comprehensive supply of cold and thermal power by using clean geothermal efficiency, but also solves the temperature imbalance caused by the attenuation of a shallow geothermal temperature field. It provides a feasible way for carbon emission reduction to realize sustainable and efficient utilization of geothermal energy.

Keywords: ORC; geothermal energy; distributed integrated energy system; heat pump; efficiency improvement



Citation: Yin, H.; Hu, L.; Li, Y.; Gong, Y.; Du, Y.; Song, C.; Zhao, J.

Application of ORC in a Distributed Integrated Energy System Driven by Deep and Shallow Geothermal Energy. *Energies* **2021**, *14*, 5466. <https://doi.org/10.3390/en14175466>

Academic Editors: Tzu-Chen Hung, Yong-Qiang Feng and Huan Xi

Received: 6 July 2021

Accepted: 18 August 2021

Published: 2 September 2021

Publisher's Note: MDPI stays neutral with regard to jurisdictional claims in published maps and institutional affiliations.



Copyright: © 2021 by the authors. Licensee MDPI, Basel, Switzerland. This article is an open access article distributed under the terms and conditions of the Creative Commons Attribution (CC BY) license (<https://creativecommons.org/licenses/by/4.0/>).

1. Introduction

With the rapid growth of global total energy consumption, global warming, ecological deterioration, and the mismatch of energy supply and demand for consumers are becoming increasingly acute [1,2]. In this context, adjustment of energy structure, utilization of renewable energies and improvement of energy efficiency are considered effective approaches for resolving the energy and environmental challenges [3]. For diminishing the carbon dioxide emissions in China, it is crucial to optimize the coal and power structure systems and vigorously develop renewable-integrated energy systems [4,5]. As a kind of renewable energy, geothermal energy reserves within 10 km of the earth's crust exceed 70,000 times of global available coal reserves [6]. Moreover, geothermal energy is not easily affected by environmental changes compared with other renewable energy such as solar energy and wind energy. As a consequence, the installed capacity utilization factor of geothermal power generation can be as high as 73%, which is approximately 1.7 times, 3.5 times, 5.2 times of hydropower, wind power and solar power generation, respectively [7].

Therefore, the development and utilization of geothermal energy is of significance for realizing the goals of the peak emissions and carbon neutrality in China by 2030 and 2060, respectively [8,9].

At present, there are two main forms [10] of utilization of geothermal energy, including the geothermal power generation and the direct utilization of geothermal energy. Specifically, typical thermal dynamic cycles are adopted for efficient power generation based on geothermal energy. In addition, the thermal energy can be also utilized for heating and cooling purposes through advanced heat exchangers, refrigeration cycle and heat pumping systems, which fulfils a diverse demand of users in energy communities. As the medium-low temperature geothermal resources are the largest reserves and are the most widely distributed geothermal energy forms [11], organic rankine cycle (ORC)-based power generation, as an effective way to utilize the medium-low temperature thermal energy, has become a current research hotspot in the field of geothermal energy utilization [12,13]. Table 1 summarizes the development status of geothermal utilization, and shallow geothermal water within 200 m is first used, represented by a ground source heat pump [14,15] and a water source heat pump [16,17]. For medium-deep geothermal utilization, the borehole heat exchanger [18], the deep downhole coaxial heat exchanger [19,20] and air conditioning [21,22] are the representatives, and the heat transfer is better. The deep geothermal temperature is high, which is suitable for geothermal power generation. ORC geothermal power generation technology is widely used [23,24]. The integrated system provides three loads of cooling, heating and power, while the independent sub-supply system can only provide a single load [25,26]. In recent years, integrated geothermal energy systems have also been widely valued. According to the statistics, the geothermal power generation is not regarded as an ideal model since the efficiency of geothermal systems for power generation is relatively low [27,28]. In order to improve the power generation efficiency or the comprehensive utilization efficiency of geothermal energy, many scholars have advanced research on the selection of system working fluids [29], operation control strategies [30], economic analysis [31], system forms [32] and theoretical models [33].

Table 1. Development of geothermal cooling, heating and power system.

System	Geothermal Source	Output/Efficiency	Time	Ref.
Heating	geothermal source heat pump	85 kW (COP = 2–3.5)	2004	[14]
	water source heat pump	105–580 kW	2020	[15]
	borehole heat exchangers	200–300 kW	2004	[16]
	deep downhole coaxial heat exchanger	700–1000 kW	2013	[17]
Cooling	air conditioning	169 kW (COP = 5.5)	2019	[18]
			2018	[19]
Power	Power generation	3949 kW	2003	[20]
			2014	[21]
Integrated system	heating-power		2021	[22]
	cooling-power	6.9–10.6%	2014	[23]
	cooling-Heating and Power		2018	[24]

For realizing a more efficient utilization of geothermal energy, this study considers the cascade utilization of geothermal energy and completely analyzes the thermal performance of deep and shallow geothermal energies. Moreover, a new type of geothermal system integrating cooling, heating and power generation is proposed. One of the characteristics is that shallow “cold” is utilized to ensure heat balance and improve system efficiency to a certain extent. In addition, the power provided by ORC here can not only generate electricity through the regulating mechanism, but also drives the compressor for refrigeration and heating. Because of the high cost of geothermal drilling, the current utilization mode is not fully utilized, resulting in a waste of energy. Using the idea of a cascade utilization

of energy, the extracted geothermal energy will be dried and squeezed. Therefore, we designed the integrated energy system based on a combination of shallow geothermal and deep geothermal, which can maximize the energy utilization. Through an innovative design, the efficient supply of “cold, heat and electricity” is realized. According to the principle of supply and demand, idle equipment is reduced. Based on the thermodynamic theory, this study analyzes the thermal efficiency of the three systems. Subsequently, the overall advantages of the system are analyzed by comparing them with the traditional independent systems which simply combine the geothermal power generation and the heat pump unit, so as to provide guidance for the comprehensive application of shallow geothermal and middle deep geothermal.

2. Geothermal-Driven Integrated Energy Systems for Buildings

A summary of geothermal utilization is shown in Figure 1. The principle of temperature matching refers to the most appropriate utilization mode of heat sources according to the temperature, which has reached the maximum energy efficiency. According to the principle of temperature matching, geothermal resources above 120 °C are used for power generation, and those between 25–120 °C are used for cooling and heating. ORC uses a low boiling point working fluid for power generation, which is very suitable for geothermal working fluid and a low temperature heat source. Geothermal heating is mainly based on a ground source heat pump and a deep heat exchanger, and the cooling with lithium bromide refrigeration as the representative. Figure 1 summarizes the influencing factors of geothermal energy, which provides a more comprehensive reference for the utilization of the comprehensive system.

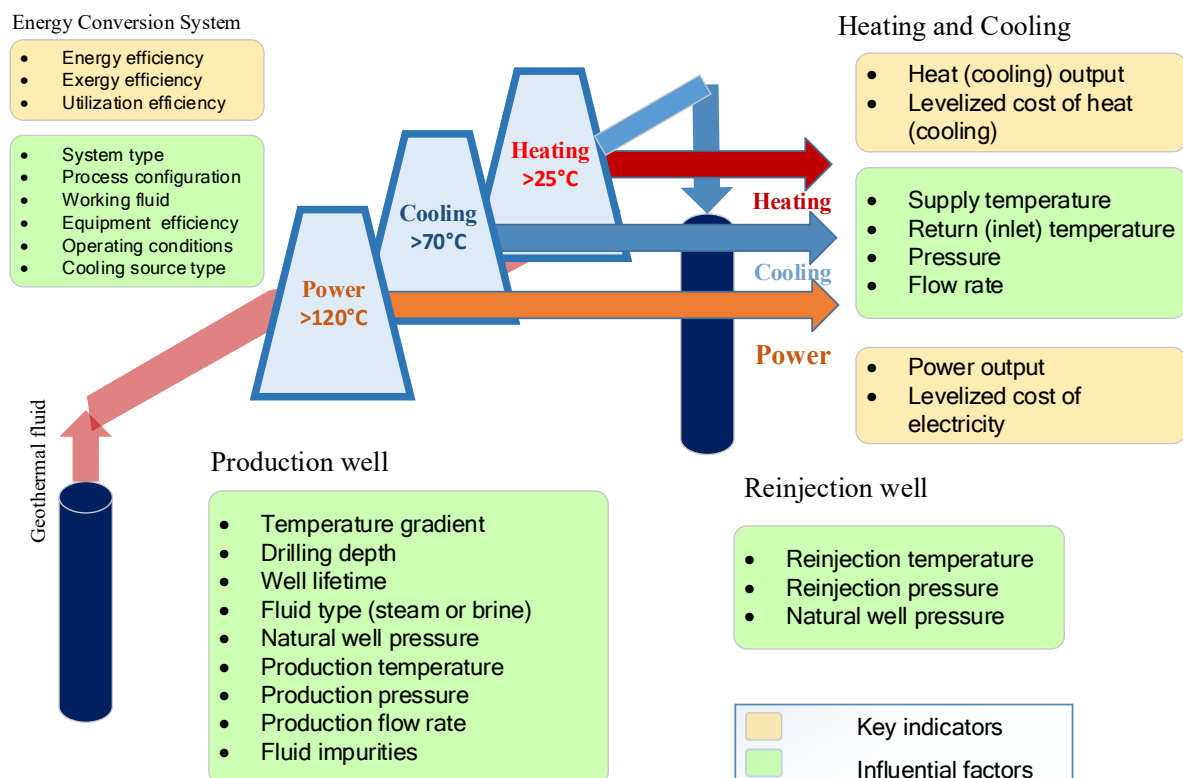


Figure 1. Influential factors and indicators for geothermal energy systems. Adapted with permission from ref. [34]. Copyright 2019 Elsevier.

The distributed integrated energy systems utilize geothermal energy in deep and shallow layers to achieve the function of cooling, heating and power supply. This is realized by coupling and by flexibly switching the Rankine forward cycle and refrigeration/heat pump reverse cycle. As a consequence, the relative balance of the annual temperature

field of the shallow geothermal well can be effectively maintained while the cold, hot and electric load of buildings can be fulfilled in different seasons. The system schematic diagram is shown in Figure 2.

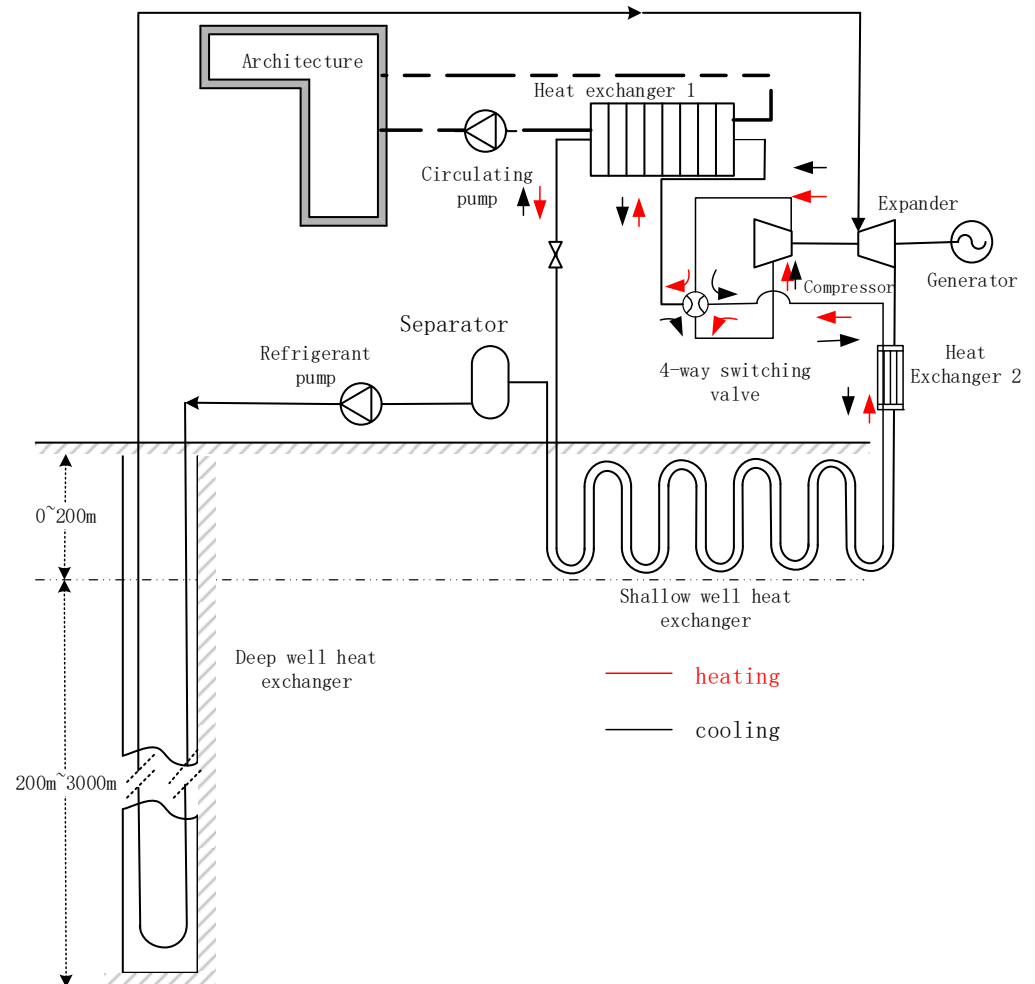


Figure 2. Schematic diagram of integrated energy system driven by geothermal energy.

The integrated energy system consists of a heat pump heating/cooling subsystem and an ORC power system. The expander is connected with a compressor by adding a coupled and coaxially connected generator at the other end. The organic working fluid in ORC power system enters the deep geothermal well to exchange heat with the underground hot water. After evaporation, the working fluid enters the expander to output the dynamic power. Next, the expander drives the generator to generate electricity. The exhaust steam is condensed in the heat exchanger in front of the well (heat exchanger 2) and the shallow heat exchanger, and then enters the gas-liquid separator. Through the working fluid pump, the liquid working fluid is pumped to the deep heat exchanger for heat absorption and evaporation, so as to complete the sub-cycle for power generation.

In the operation of the refrigeration subsystem, the expander in the original power generation subsystem drives the compressor to compress the gaseous refrigerant by switching the coupling unit. The compressed high-temperature and high-pressure refrigerant enters the shallow heat exchanger through the four-way reversing valve to release heat and is condensed into the subcooled state. After throttling by the throttle valve, the refrigerant evaporates and absorbs heat in the user side heat exchanger (which is now used as the evaporator) to cool the cold water and provides cold to the user as required. After evaporation, the gaseous refrigerant enters the compressor for compression to complete the sub-cycle of refrigeration. Similarly, during the operation of the heating subsystem, the expander in

the original power subsystem drives the compressor to compress the gaseous refrigerant. The refrigerant with the high temperature and high pressure is exchanged through the four-way reversing valve and then enters the user side heat exchanger (heat exchanger 1, which is now used as the condenser) to exchange heat with the hot water on the user side. Due to the heat absorption, the hot water can be later utilized for meeting the heat demand on the user side. It is pointed out that the net output of mechanical power, heat and cold can be flexibly adjusted by coupling the heat pump heating/cooling subsystem and ORC power generation subsystem. In addition, the coupled heat exchangers of the two subsystems include the heat exchanger 2 and the shallow heat exchanger. For heat and power co-generation in winter, the heat exchanger 2 and the shallow heat exchanger are used as the condenser of the power generation system and the evaporator of the heating subsystem, respectively.

3. Thermodynamic Model for the Integrated Energy System

3.1. Preliminary Selection of the Working Fluid

For the thermal cycle, in addition to cycle conditions, the working fluid has an extremely important influence on the cycle performance [35–37]. Whether for refrigeration cycle working fluids (A) or for ORC working fluids (B), the physical parameters, the safety and environmental performance of working fluid should be comprehensively considered. The basic assumptions are as below [38,39]:

- (1) The solidification temperature is lower than the lowest possible temperature of the cycle, and the triple point temperature is lower than the ambient temperature.
- (2) It has a good thermal conductivity and a low viscosity.
- (3) No corrosion, no combustion and stable chemical properties.
- (4) Ozone depletion potential (ODP) is zero and global warming potential (GWP) is low.
- (5) No toxicity to the human body.

In the premise of the above, the five most commonly used working fluids in the industry are preliminarily selected as the circulating working fluids for the two subsystems, and the optimal working fluids corresponding to the two subsystems are determined based on the thermodynamic analysis. The specific parameters of the five working fluids are shown in Table 2.

Table 2. Physical parameters of the five primary selected working fluids.

Working Fluid	Critical Temperature (°C)	Molecular Weight (kg/kMOL)	Molecular Formula	Standard Boiling Point (°C)	Critical Pressure (MPa)	ODP	GWP
R134a	101.06	102.03	C ₂ H ₂ F ₄	−26.07	4.06	0	1300
R152a	113.26	66.05	C ₂ H ₄ F ₂	−24.02	4.52	0	124
R236ea	139.29	152.04	CF ₃ CHFCHF ₂	6.17	3.42	0	710
R245fa	154.01	134.05	CF ₃ CH ₂ CHF ₂	15.14	3.65	0	950
R245ca	174.42	134.05	CHF ₂ CF ₂ CH ₂ F	25.26	3.94	0	560

3.2. System Hypothesis and Parameter Setting

In the deep and shallow geothermal energy system, the refrigeration cycle subsystem is set as a vapor compression refrigeration cycle. Because most of the high-temperature geothermal energy discovered in China is between 120–180 °C, it has a medium–high temperature, and the subcritical cycle is more applicable. To simplify the model, the following assumptions are adopted for the thermodynamic calculation of the integrated system:

- (1) The system works stably.
- (2) The heat loss and pressure loss in the thermodynamic process of the system are not considered.
- (3) The efficiency of mechanical equipment is calculated according to the conventional equipment parameters (as shown in Table 3).

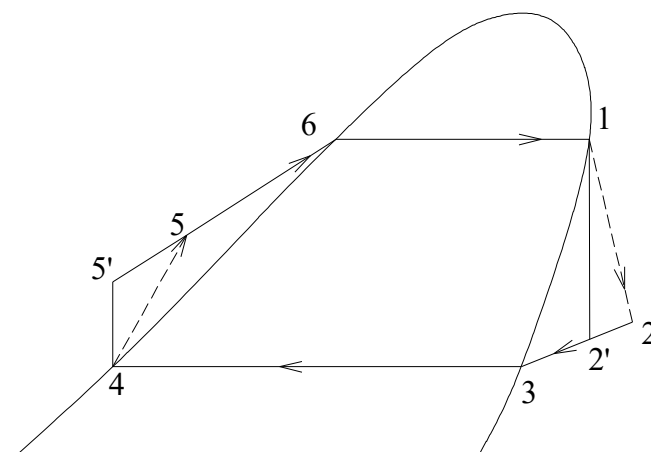
Table 3. Parameter setting of integrated energy system.

Parameter	Symbol	Unit	Set Value
Mass flow rate of working fluid B	m_B	kg/s	15
Isentropic efficiency of the compressor	η_{comp}	%	75
Isentropic efficiency of the working fluid pump	η_{pum}	%	80
Relative internal efficiency of the expander	η_{tur}	%	80
Transmission mechanical efficiency	η_c	%	90
Generator efficiency	η_{motor}	%	95
Geothermal temperature of the shallow well	T_L	°C	18
Outlet temperature of working fluid B in the deep well	T_H	°C	120
Cold water inlet temperature	T_{in-l}	°C	12
Cold water outlet temperature	T_{out-l}	°C	7
Hot water inlet temperature	T_{in-h}	°C	45
Hot water outlet temperature	T_{out-h}	°C	50

In order to reflect the power generation and refrigeration and heating performance of the system, the total thermal efficiency of the system η_{net} is selected as its evaluation index.

3.3. Thermodynamic Calculation of the Coupling System

In summer cooling or winter heating seasons, the coupling is adjusted according to the cooling and heating load (compressor power consumption), and the expander output power beyond the compressor load is used to drive the generator to generate electricity. In transitional seasons, since there is no heating and cooling demand on the user side, the system uses all the expansion work for electricity generation by disconnecting the coupling between the compressor and the expander, which is used to supply power for electrical equipment in buildings or transmittance to the grid. The thermodynamic process of the ORC system is shown in Figure 3. Here, 6-1 is heat absorbing process in deep well heat exchanger. Then 1-2' is isentropic expansion, and 1-2 is the actual expansion process in the expander. 2-3-4 indicates that the condensation process is in heat exchanger 2 and shallow well heat exchanger. 4-5-6 indicates the process that the refrigerant pump sends the liquid working medium back to the deep well heat exchanger. Then, a power generation cycle is completed.

**Figure 3.** T-S diagram of thermodynamic process of subcritical ORC.

In the analysis, the work done by the working fluid in the expander is W_{ORC} :

$$W_{ORC} = m_B(h_1 - h_2) = m_B(h_1 - h_{2'})\eta_{turb} \quad (1)$$

where h_1 and h_2 are enthalpy values at the inlet and outlet of the expander, kJ/(kg·K).

The heat absorbed by the condenser (shallow heat exchanger and heat exchanger 2) is Q_L :

$$Q_L = m_B(h_2 - h_4) \quad (2)$$

where h_4 is the enthalpy at the condenser outlet, kJ/(kg·K).

The heat absorbed by the working fluid in a deep heat exchanger in the ORC cycle is written as Q_H :

$$Q_L = m_B(h_2 - h_4) \quad (3)$$

The power consumption of the working fluid in the pump is represented by W_{pump} :

$$W_{pump} = m_B(h_5 - h_4) = \frac{m_B(h_{5'} - h_4)}{\eta_{pump}} \quad (4)$$

where h_5 is the ideal enthalpy at the outlet of the working medium pump, kJ/(kg·K).

Assuming that the working fluid B is dry-saturated steam with a temperature of 120 °C at the outlet of the deep heat exchanger and enters the expander at this state, the above parameters can be calculated according to the enthalpy value of working fluid at each state point in the T-S diagram.

In winter or summer, the user side will need heating and cooling. As a result, the coupling between the expander and the compressor can be connected to make part of the output power of the expander to drive the compressor for a refrigeration and compression cycle. The thermodynamic process of the cycle is shown in Figure 4. In the refrigeration conditions, the refrigerant evaporated by heat exchanger 1 turns into steam (8), adiabatically compressed into high-temperature and high-pressure steam (9) by a compressor, condensed into state 12 by heat exchanger 2 and a shallow geothermal heat exchanger, throttled by a throttle valve, turns it into a gas-liquid mixture (13), and enters heat exchanger 1 to absorb heat and provide a cooling capacity for users. In the heating condition, the steam (8) from the shallow geothermal heat exchanger changes into high-temperature and high-pressure steam (9) after adiabatic compression by the compressor enters heat exchanger 1 through the four-way valve for condensation, provides heat for the user, changes into liquid 12 after heat release, changes into a gas-liquid mixture (13) through the throttle valve, and enters the shallow geothermal heat exchanger for heat absorption to complete a heating cycle.

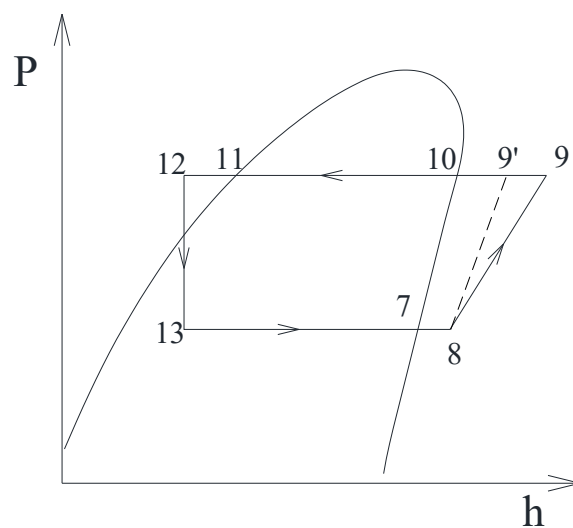


Figure 4. P-h diagram of the thermodynamic process of the refrigeration/heat pump cycle.

After evaporation, the vapor of refrigerant A is sucked into the suction port of the compressor for compression, and the power consumption of the compressor is as follows:

$$W_{comp} = m_A(h_9 - h_8) = \frac{m_A(h_{9'} - h_8)}{\eta_{comp}} \quad (5)$$

where η_{comp} is the isentropic efficiency of the compressor.

The high temperature exhaust of the compressor condenses and releases heat in the heat exchanger (heat demand side or condenser), and its condensing heat load or heating capacity Q_C can be calculated by the following Formula:

$$Q_C = m_A(h_9 - h_{12}) \quad (6)$$

The thermal efficiency of the whole cycle system η_{net} is as follows:

$$\eta_{net} = \frac{W_{ORC}}{Q_H} \quad (7)$$

Cop of refrigeration or heating is equal to the ratio of the condensing heat load or heating load to compressor power consumption under corresponding working conditions:

$$COP = \frac{Q_c}{W_{comp}} \quad (8)$$

The above parameters are obtained by NIST calling the enthalpy and entropy of the corresponding parameters.

4. Analysis of Cycle Calculation Results

According to the cycle efficiency and the heat absorption and discharge data of the related heat exchanger, the integrated energy system was compared with the traditional energy supply system in terms of the heat balance of the ground heat storage, the efficiency of power generation and refrigeration and heating.

4.1. Thermal Characteristics of the Integrated Energy System Based on Geothermal Wells

In consideration of the regional climate differences, North China is taken as an example in the study (the heating period in winter is generally from November to February of the next year, and in summer is generally from July to September). Under the condition of fixed deep and shallow geothermal parameters, three operation modes can be divided according to the actual seasonal demand:

- (1) Winter heating and power generation mode (set the annual operation hours as 3000 h): in this mode, the output power of the expander can not only meet the heating requirements required to drive the compressor, but also the remaining expansion work can be used to drive the generator for power generation.
- (2) Summer refrigeration and power generation mode (set the annual operation hours as 2000 h): in this mode, the output power of the expander can not only meet the refrigeration requirements required to drive the compressor, but also the remaining expansion work can be used to drive the generator for power generation. The simulation results show that in summer, the refrigerant condenses in the shallow heat exchanger. Because the temperature of the shallow well is lower than the ambient temperature in summer, the pressure ratio of the compressor decreases with the decrease of the condensation temperature, which improves the COP of the refrigeration cycle.
- (3) Transition season power generation mode (set the annual operation hours as 3000 h): in this mode, there is no demand for cooling and heating on the user side. At this time, the coupling between the compressor and the expander is disconnected, and all the output power of the expander is used for the generator power generation. The generated electricity is not only used for the system's own use, but also for the grid.

The setting parameters of the three operating modes are shown in Table 4.

Table 4. Main operation parameter settings of the three modes.

Category		Heating and Power Generation	Refrigeration and Power Generation	Independent Generation
Annual operating hours		2000 h	3000 h	3000 h
ORC system	Inlet temperature of the expander	120 °C	120 °C	120 °C
	Condensation temperature of the shallow well	30 °C	40 °C	40 °C
Isentropic efficiency of the compressor		0.75	0.75	/
Heating and cooling system	Evaporation temperature	11 °C	5 °C	/
	Inspiratory temperature	16 °C	7 °C	/
	Condensation temperature	52 °C	25 °C	/

The COP of the refrigeration and heating cycle and the thermal efficiency of ORC under the above conditions (condensation temperature and evaporation temperature) using the five working fluids in Table 2 are calculated and compared. The specific results are shown in Figures 5–7.

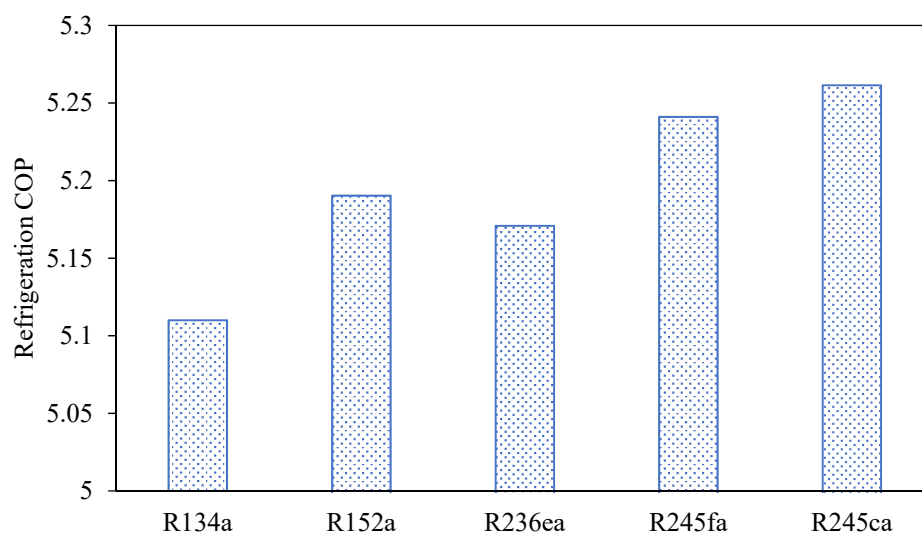


Figure 5. COP comparison of different refrigerants in the refrigeration cycle.

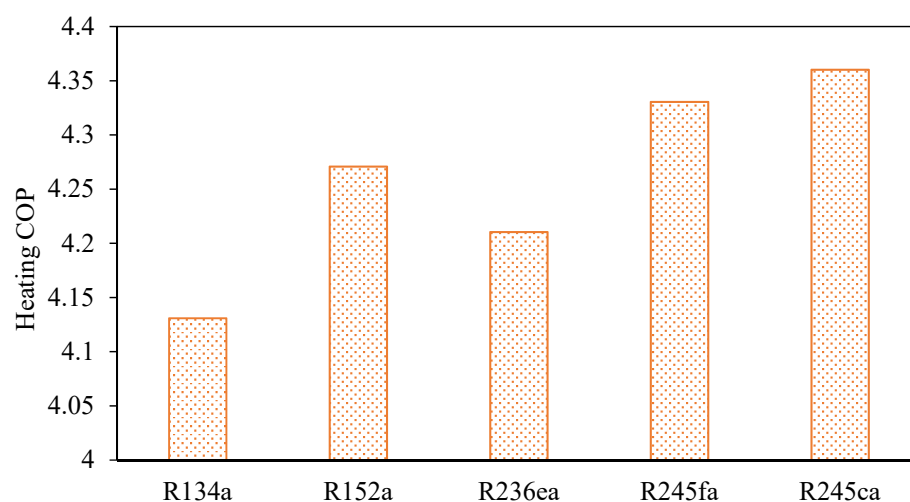


Figure 6. COP comparison of different refrigerants on heating cycle.

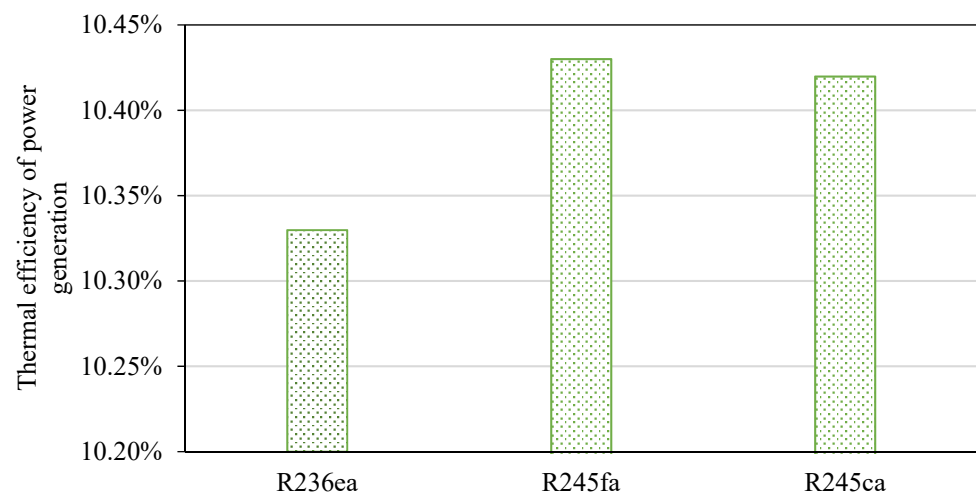


Figure 7. Generation efficiency comparison of the different refrigerants.

In the power generation subsystem, when the evaporation temperature is 120 °C, it exceeds the critical temperatures of R134a and R152a. This paper only discusses the subcritical ORC, so the two working fluids are not discussed. Only the last three working fluids are analyzed. The comparison of thermal efficiency is shown in Figure 7 below.

According to the comparison of the above figures, for the heating/cooling subsystem, the optimal working fluid is R245ca, and the COP of refrigeration and heating is 5.26 and 4.36, respectively. For the ORC subsystem, by comparing the operating thermal efficiency of the three working substances, it is found that R245fa is the optimal working fluid with a thermal efficiency of 10.43%. Therefore, R245ca is selected as a working fluid for heating/cooling subsystem and R245fa is selected as a working fluid for the ORC subsystem.

Based on the established thermodynamic model and the selected working fluid, the main operating parameters of the three modes can be calculated. The specific simulation data are shown in Table 5.

Table 5. Outputs of the coupling energy system in typical operation modes.

Category	Refrigeration and Power Generation	Heating and Power Generation	Independent Generation
Heat absorption of the deep well (kW)	3810	4020	3827
Output work (kW)	399	489	399
Thermal efficiency (%)	10.47	12.18	10.43
Annual heat-obtaining quantity of the shallow well (kJ)	3.11×10^{10}	1.85×10^{10}	3.62×10^{10}

By analyzing the calculation data, it can be seen that the thermal efficiency of the system in the winter heating mode is 12.18%, which is significantly higher than that in the refrigeration and power generation mode (10.47%) and that in the independent generation mode (10.43%). The thermal efficiency is 1.7% higher than that of the two modes, indicating a relative improvement of approximately 16%. The reason is that under the heating and power generation mode, the refrigerant evaporates in the shallow heat exchanger, and the low temperature R245ca working fluid exchanges heat with R245fa in the ORC system in heat exchanger 2. As a result, the suction temperature of the compressor is increased, while the exhaust steam temperature is reduced, which is beneficial for the operation of the heat pump. In addition, because the refrigerant evaporates in the shallow heat exchanger, the condensing temperature of the ORC system can be reduced, leading to an increase in the output work by the expander and an improvement in the overall thermal efficiency of the system.

According to Table 4, the annual heat-obtaining quantity of the shallow geothermal well Q_{total} is as follows:

$$Q_{total} = Q_{cold} + Q_{heat} + Q_{power} \quad (9)$$

In which, Q_{cold} is the heat-obtaining quantity of the shallow geothermal well in cooling and power generation mode, Q_{heat} is the heat-obtaining quantity of the shallow geothermal well in the heating and power generation mode, and Q_{power} denotes the heat-obtaining quantity of the shallow geothermal well in the independent power generation mode. In the analysis, the annual heat-obtaining quantity Q_{total} is calculated as 8.58×10^{10} kJ.

In the instance that the coupling system is not applied, the heat-obtaining quantity of the shallow well Q'_{total} in the annual independent power generation mode is as follows:

$$Q'_{total} = Q_{power} \times \frac{\tau_{total}}{\tau_{power}} \quad (10)$$

where τ_{power} is the operation hours of the independent power generation in the transition seasons of the coupling system, and τ_{total} represents the operation hours of the whole system in the whole year. The calculated heat-obtaining quantity Q'_{total} is 9.66×10^{10} kJ.

By analyzing the heat gain results of the shallow geothermal well in the two cases, it is found that the annual heat-obtaining quantity of the shallow geothermal well (8.58×10^{10} kJ) is 11.18% lower than that of the independent power generation (9.66×10^{10} kJ). This is due to the coupling heat transfer of two subsystems in the shallow geothermal well. It is speculated that the integrated energy system can better maintain the balance of the annual temperature field of the shallow geothermal reservoir.

4.2. Comparative Analysis of the Distributed Integrated Energy System with Traditional Independent Distribution Systems

The simulation results show that under the heating mode in winter, the working fluid evaporates in the shallow well heat exchanger, and the refrigeration working fluid and ORC working fluid exchange heat in the shallow well front heat exchanger, thus reducing the exhaust steam temperature and increasing the suction temperature of the compressor.

This has three beneficial effects: (1) the annual temperature field balance of shallow geothermal energy is effectively maintained; (2) the refrigerant evaporates in the shallow well heat exchanger, reducing the condensation temperature of ORC system, thus increasing the output power of expander; (3) the refrigerant evaporates in the shallow well heat exchanger, and the evaporation temperature is higher (the shallow water temperature is significantly higher than the air or ambient temperature in winter). The COP of refrigeration is therefore improved.

As shown in Figure 8, the annual cooling output (2000 h in refrigeration season) of the integrated energy system is 5.31×10^9 kJ, and the annual heating output (3000 h in refrigeration season) of the integrated energy system is 1.47×10^{10} kJ, while the annual generating output of the system (in which the independent generation mode is calculated according to the transition seasons of 3000 h) is 6.76×10^9 kJ. In the condition that geothermal energy is regarded as the single heat source for ORC throughout the year, the total annual power generation (calculated at 8000 h) is 9.82×10^9 kJ. In order to meet the demand of refrigeration and heating, it is assumed that the refrigeration and heating units adopt the traditional heat pump units. According to the COP performance level of the industry, the refrigeration COP is 3.8 and the heating COP is 4.5. For the same cold and heat production, the power consumption is 1.40×10^9 kJ and 3.26×10^9 kJ, respectively.

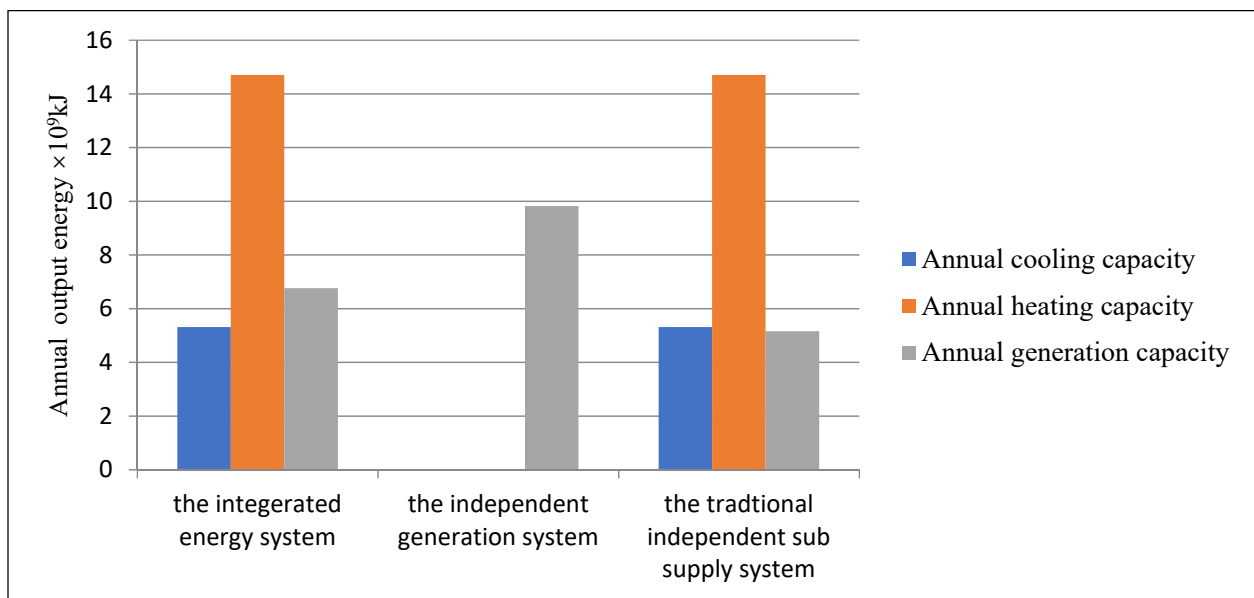


Figure 8. Comparison between the integrated energy system and independent sub supply system.

Therefore, the net power generation of the independent power distribution system of the geothermal power generation–heat pump unit is 5.17×10^9 kJ after removing the power consumption of refrigeration and heating. In this paper, the cycle net power generation of the integrated energy system is calculated to be 6.76×10^9 kJ, which is 1.59×10^9 kJ more than that of the traditional independent sub supply system and nearly 31% higher than that of the control group. From the perspective of the energy system, an integrated energy system has great advantages.

5. Outlook on ORC in the Distributed Integrated Energy System Driven by Deep and Shallow Geothermal

In view of the sustainable characteristics of geothermal energy and the conformation of the distributed integrated geothermal systems to the principle of energy cascade utilization and temperature matching, the regional energy station based on a distributed integrated energy system driven by deep and shallow geothermal energy is expected to become one of the alternative paths for the carbon emission reduction. It is worth mentioning that the promotion of the system performance is highly dependent on the breakthrough of ORC technology. As illustrated, although the ORC technology has been applied for power generation using low temperature heat sources for a long time, the round-trip efficiency of energy systems is still restrained within 15% based on the latest statistics. Great efforts have been made to improve the thermal performance of geothermal systems in the following aspects:

(1) The collaborative matching of the evaporation temperature and thermophysical properties of the heat source and the organic working fluid. Although geothermal energy is more stable than other renewable energy sources, in the long run, the heat-taking temperature has a chronic decay; therefore, the method for matching the heat source temperature and the evaporation temperature need to be established. (2) The evaluation indicator of the ORC system in consideration of thermal performance and environmental impact. The design of geothermal systems and the selection of organic working fluids are the main trend of the ORC technology development towards high thermal performance, low carbon emission and safe operation. (3) Turbine development. Despite the difficulties in research and development, the turbine deliberately invented for ORC systems are a significant factor to be considered. The specific path is shown in Figure 9.

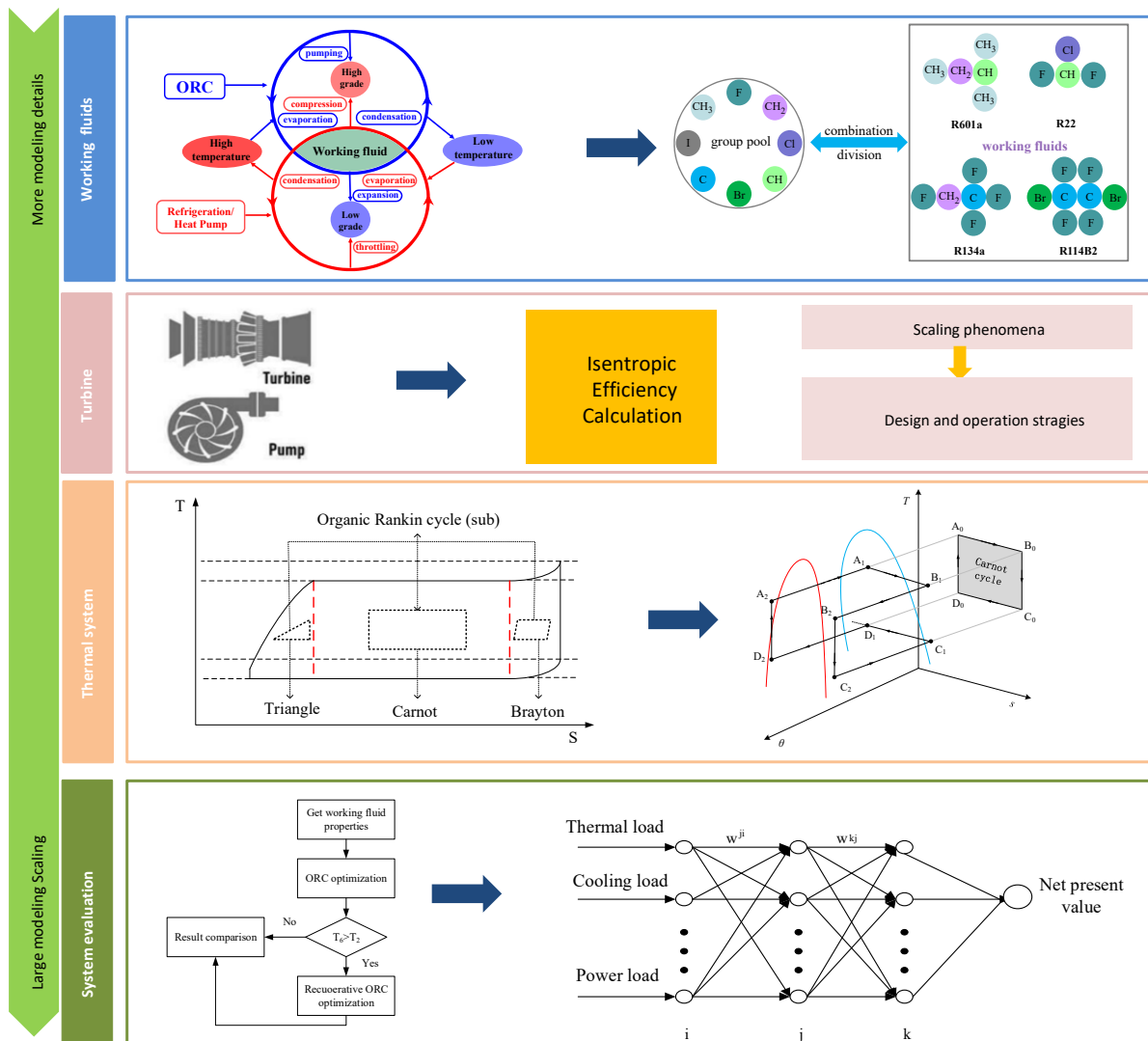


Figure 9. Multi-scale modeling and optimization framework of ORC for the geothermal energy systems.

6. Conclusions

This study presents an integrated system innovatively, which realizes the comprehensive supply of cold and thermal power by using clean geothermal efficiency, but also solves the temperature imbalance caused by the attenuation of a shallow geothermal temperature field. Based on the thermodynamic theory, this study analyzes the thermal efficiency of the three systems. The conclusions are as follows:

- (1) In the heating and power generation mode, the thermal efficiency of the integrated energy system is 12.18%, which is significantly higher than that in the cooling and power generation mode and the single power generation mode. The efficiency increase rate is 16%.
- (2) The annual heat-obtaining quantity of the shallow geothermal well of the established integrated energy systems is 11.18% lower than that obtained by single power generation, indicating that the integrated energy system can better maintain the balance of an annual temperature field of shallow geothermal energy.
- (3) Compared with the traditional independent sub supply system (only using geothermal power generation and heat pump units throughout the year), the integrated energy system generates 1.59×10^9 kJ more electricity per year, which is approximately 31% higher.

Through an innovative design, the efficient supply of “cold, heat and electricity” is realized. According to the principle of supply and demand, idle equipment is reduced. Despite the superiority of the integrated system in sustainability and efficiency, it is critical to analyze the economics between the integrated system and the independent distribution system in the next work.

Author Contributions: Conceptualization, H.Y.; methodology, L.H.; formal analysis, Y.D.; investigation, C.S.; writing—original draft preparation, H.Y. and L.H.; writing—review and editing, H.Y.; supervision, Y.L., J.Z. and Y.G. All authors have read and agreed to the published version of the manuscript.

Funding: This research was funded by Key research and development project in Tianjin (20YFYSGX00020), Science and technology service network initiative of Chinese academy of sciences (KFJ-STQ-QYZD-2021-02-006).

Conflicts of Interest: The authors declare no conflict of interest.

References

1. Takada, H.H.; Ribeiro, C.O.; Costa, O.L.; Stern, J.M. Gini and Entropy-Based Spread Indexes for Primary Energy Consumption Efficiency and CO₂ Emission. *Energies* **2020**, *13*, 4938. [[CrossRef](#)]
2. Martins, F.; Felgueiras, C.; Smítková, M.; Caetano, N. Analysis of Fossil Fuel Energy Consumption and Environmental Impacts in European Countries. *Energies* **2019**, *12*, 964. [[CrossRef](#)]
3. Clauser, C.; Ewert, M. The renewables cost challenge: Levelized cost of geothermal electric energy compared to other sources of primary energy—Review and case study. *Renew. Sustain. Energy Rev.* **2018**, *82*, 3683–3693. [[CrossRef](#)]
4. Lilin, X.; Lan, X. Understanding and suggestions on the formulation of China’s energy low carbon “14th five year plan” and working fluid and long term development plan. *Int. Pet. Econ.* **2020**, *28*, 1–10.
5. Yunzhou, Z.; Hongcai, D.; Xiaoyu, W.; Rui, C.; Ning, Z. Development trend and key issues of integrated energy services in China. *China Electr. Power* **2021**, *54*, 1–10.
6. Wang, G.L.; Zhang, W.; Liang, J.Y.; Lin, W.J.; Liu, Z.M.; Wang, W.L. Evaluation of geothermal resources potential in China. *Acta Geosci. Sin.* **2017**, *4*, 449–450.
7. Zhu, J.; Hu, K.; Lu, X.; Huang, X.; Liu, K.; Wu, X. A review of geothermal energy resources, development, and applications in China: Current status and prospects. *Energy* **2015**, *93*, 466–483. [[CrossRef](#)]
8. Wei, G.; Renhu, T. Electric power industry under 2060 carbon neutral target. *Energy* **2020**, *142*, 14–21.
9. Xian, L.Z.; Rui, L.; Hao, G.; Fengnian, Z. Spatial analysis of geothermal industry development in China. *Int. Pet. Econ.* **2021**, *29*, 40–47.
10. Tianshu, T.; Huimin, W.; Jiachao, H.; Xiaohan, Z. Analysis on utilization status and development opportunities of geothermal energy in China. *J. Petrochem. Manag. Cadre Coll.* **2020**, *22*, 62–66.
11. Jinhua, Z.; Wei, W.; Dong, D.; Xinghua, W.; Pei, W. Development, utilization and sustainable development of geothermal resources. *Sino Foreign Energy* **2013**, *18*, 30–35.
12. Chao, L.; Jinliang, X. Selection of ORC working fluids for medium and low temperature geothermal power generation. *Renew. Energy* **2014**, *32*, 1188–1194.
13. Hongwei, G.; Pengfei, Y.; Chao, Z.; Jie, Y. Thermal economy analysis of subcritical ORC power generation system. *J. Tianjin Univ. Technol.* **2020**, *36*, 31–35.
14. Hepbasli, A.; Akdemir, O. Energy and exergy analysis of a ground source (geothermal) heat pump system. *Energy Convers. Manag.* **2004**, *45*, 734–753. [[CrossRef](#)]
15. Maddah, S.; Goodarzi, M.; Safaei, M.R. Comparative study of the performance of air and geothermal sources of heat pumps cycle operating with various refrigerants and vapor injection. *AEJ-Alex. Eng. J.* **2020**, *59*, 4037–4047. [[CrossRef](#)]
16. Jung, Y.; Kim, J.; Kim, H.; Nam, Y.; Cho, H.; Lee, H. Comprehensive multi-criteria evaluation of water source heat pump systems in terms of building type, water source, and water intake distance. *Energy Build.* **2021**, *236*, 110765. [[CrossRef](#)]
17. Deng, Z. Modeling of Standing Column Wells in Ground Source Heat Pump Systems. Ph.D. Thesis, Oklahoma State University, Stillwater, OK, USA, 2004.
18. Dijkshoorn, L.; Speer, S.; Pechinig, R. Measurements and Design Calculations for a Deep Coaxial Borehole Heat Exchanger in Aachen, Germany. *Int. J. Geophys.* **2013**, *2013*, 14. [[CrossRef](#)]
19. Dai, C.; Li, J.; Shi, Y.; Zeng, L.; Lei, H. An experiment on heat extraction from a deep geothermal well using a downhole coaxial open loop design. *Appl. Energy* **2019**, *252*, 113447. [[CrossRef](#)]
20. LMa; Zhao, Y.; Yin, H.M.; Zhao, J.; Li, W.; Wang, H. A coupled heat transfer model of medium -depth downhole coaxial heat exchanger based on the piecewise analytical solution. *Energy Convers. Manag.* **2019**, *204*, 112308.
21. Frau, C.; Maggio, E.; Poggi, F.; Melis, E.; Floris, F.; Orrù, P.F. Low-enthalpy geothermal systems for air conditioning: A case study in the Mediterranean climate. *Energy Procedia* **2018**, *148*, 527–534. [[CrossRef](#)]

22. Dang, X.Y.; Lei, F.; Wang, F. An Analysis of the Technique and Economics of the Geothermal-Source Heat Pump Air-Conditioning System. *J. Appl. Sci.* **2003**, *21*, 377–380.
23. Guzovic, Z.; Raskovic, P.; Blataric, Z. The comparison of a basic and a dual-pressure ORC (ORC): Geothermal Power Plant Velika Ciglena case study. *Energy* **2014**, *76*, 175–186. [[CrossRef](#)]
24. Coskun, A.; Bolatturk, A.; Kanoglu, M. Thermodynamic and economic analysis and optimization of power cycles for a medium temperature geothermal resource. *Energy Convers. Manag.* **2014**, *78*, 39–49. [[CrossRef](#)]
25. Pastor-Martinez, E.; Rubio-Maya, C.; Ambriz-Diaz, V.M.; Belman-Flores, J.M.; Pacheco-Ibarra, J.J. Energetic and exergetic performance comparison of different polygeneration arrangements utilizing geothermal energy in cascade. *Energy Convers. Manag.* **2018**, *168*, 252–269. [[CrossRef](#)]
26. DiPippo, R. Geothermal power plants: Evolution and performance assessments. *Geothermics* **2015**, *53*, 291–307. [[CrossRef](#)]
27. Nieves, O.; Nancarrow, T.; Mackinnon, J. A meta-study of the effect of thermodynamic parameters on the efficiency of geothermal power plants worldwide. *PAM Rev. Energy Sci. Technol.* **2016**, *3*, 27–28. [[CrossRef](#)]
28. Zhonghe, H.; Yan, D.; Zhi, W. Selection of working medium for low temperature waste heat recovery system of ORC. *Prog. Chem. Ind.* **2014**, *33*, 2279–2285.
29. Luyao, T. *Optimal Operation Strategy of Ground Source Heat Pump Coupled with Cold and Heat Sources*; Beijing Jianzhu University: Beijing, China, 2020.
30. Hongjiu, R.; Sumin, Z. Analysis on the main controlling factors of geothermal heating economy-Taking Tianjin as an example. *China Land Resour. Econ.* **2018**, *31*, 41–45.
31. Boyaghchi, F.A.; Chavoshi, M.; Sabeti, V. Optimization of a novel combined cooling, heating and power cycle driven by geothermal and solar energies using the water/CuO (copper oxide) nanofluid. *Energy* **2015**, *91*, 685–699. [[CrossRef](#)]
32. Xu, Q.; Gong, Y.; Luo, C.; Yao, Y.; Lu, Z.; Ma, W. Research progress of solar geothermal power generation system. *New Energy Prog.* **2016**, *5*, 404–410.
33. Zhao, J.; Hu, L.; Wang, Y.; Yin, H.; Deng, S.; Li, W.; Du, Y.; An, Q. How to Rapidly Predict the Performance of ORC: Optimal Empirical Correlation based on Cycle Separation. *Energy Convers. Manag.* **2019**, *188*, 86–93. [[CrossRef](#)]
34. Lee, I.; Tester, J.W.; You, F. Systems analysis, design, and optimization of geothermal energy systems for power production and polygeneration: State-of-the-art and future challenges. *Renew. Sustain. Energy Rev.* **2019**, *109*, 551–577. [[CrossRef](#)]
35. Linke, P.; Papadopoulos, A.I.; Seferlis, P. Systematic Methods for Working Fluid Selection and the Design, Integration and Control of ORCs—A Review. *Energies* **2015**, *8*, 4755–4801. [[CrossRef](#)]
36. Costante, I.; Nadeem, S. High-Efficiency Small-Scale Combined Heat and Power Organic Binary Rankine Cycles. *Energies* **2018**, *11*, 994.
37. Saboor, K.; Nasser Mohammed, A.; ManHoe, K. Thermodynamic Study of a Combined Power and Refrigeration System for Low-Grade Heat Energy Source. *Energies* **2021**, *14*, 410.
38. Huijun, L.; Kaina, G.; Chao, M. Selection of organic working fluids for power generation based on different temperature heat sources. *Steam Turbine Technol.* **2013**, *55*, 251–254.
39. Peng, L.; Zhonghe, H.; Zhongkai, M.; Xu, H.; Zhi, W. Low temperature superheated ORC working fluid selection and parameter optimization. *Acta Sol. Energy Sin.* **2018**, *39*, 2393–2402.